Available online at www.sciencedirect.com
SCIENCE DIRECT
Polymer 47 (2006) 4603–4612
polymer
www.elsevier.com/locate/polymer

Low VOC bifunctional photoinitiator based on α-hydroxyalkylphenone structure

Guodong Ye [a,b], Zhuofeng Ke [a], Jianwen Yang [a], Tianyi Zhao [a], Zhaohua Zeng [a,*], Yonglie Chen [a]

[a] School of Chemistry and Chemical Engineering, Institute of Polymer Science, Sun Yat-Sen University, Guangzhou 510275, People's Republic of China
[b] Department of Chemistry, Guangzhou Medical College, Guangzhou 510182, People' Republic of China

Received 3 October 2005; received in revised form 4 March 2006; accepted 23 April 2006
Available online 16 May 2006

Abstract

A novel bifunctional photoinitiator (PI), bis[4-(2-hydroxy-isopropionyl)]ether (BHPE), was synthesized and characterized. Photophysics investigation showed that the absorption maximum of BHPE was at 281 nm, red shifted about 40 nm compared to the commercial photoinitiators 2-hydroxy-2-methyl-1-phenyl-propan-1-one (HMPP) and 1-hydroxycyclohexyl phenyl ketone (HCPK), dropping into the UVB region, and the fluorescence lifetime and fluorescence quantum yields of BHPE were found to be 14.2 ns and 0.045, respectively. The photoinitiating activity of BHPE was tested in comparison with HMPP by means of differential photo-calorimetry (DPC or Photo-DSC), and the initiation efficiency of BHPE was found to be comparable to that of HMPP. Bond dissociation enthalpy (BDE) of BHPE was calculated by quantum chemistry with the B3LYP method of 6-311++G** basis sets and found to be 67.8 kcal/mol, very close to that of HMPP (65.0 kcal/mol) and HCPK (63.5 kcal/mol). The quantum yields of initiation and polymerization were determined to be 58 and 296 for BHPE, 100 (defined as reference) and 389 for HMPP, respectively. A photochemical mechanism was proposed based on the results of steady-state photolysis UV spectra, GC–MS, NMR and GPC. Volatility of BHPE was tested under simulated outdoor conditions, showing very low volatility comparing to the corresponding commercial photoinitiator. Results showed that BHPE is a promising candidate as a PI with reduced VOC emission.

Keywords: Photoinitiator; VOC; UV-curing

1. Introduction

Photoinitiators (PIs) bearing α-hydroxyalkylphenone structure, such as HMPP, HCPK and HHMP (Scheme 1), are widely used as commercial photoinitiators for initiating free radical photopolymerization of acrylate/vinyl monomers or oligomers in radiation curing technology [1–6]. They are highly photo activity with high thermal stability and good coloring characteristics in clear coatings. The physicochemical and photophysical properties of α-hydroxyalkylphenone PIs were widely investigated [7–13], and relatively high activity in initiating free radical photopolymerization was found. However, one of the critical issues for this kind of photoinitiators in UV-curing process is that their photodecompose products or their undecomposed molecules may migrate from the cured matrix to the surface or release to atmosphere. This may cause VOC problem and induce difficulty for UV-curable formulations in application in food, medicine and pharmaceutical packaging.

Traditional monofunctional photoinitiators suffer from VOC problem due to their low molecular weight. For example, HMPP is a liquid with boiling point of about 105 °C, and can generate benzaldehyde in photodecomposition, which is odorous and harmful to health. The development of macrophotoinitiators is one of the approaches to solve the problem. One example is Esacure KIP 150 (Scheme 1), which was developed and commercialized by Lamberti. The photoinitiating activity of KIP 150 can basically satisfy the application in UV-curing formulation, but the cured film based on it is often rigid and brickle because of the α-methyl styrene backbone in KIP 150. Another disadvantage of this approach is that for most of photoinitiators the photoinitiating activity will descend in some degree as they are immobilized to the macromolecular backbone.

In this paper, a novel photoinitiator with two photoactive groups based on α-hydroxyalkylphenone structure had been

* Corresponding author. Tel.: +86 20 84111138.
E-mail address: ceszzh@zsu.edu.cn (Z. Zeng).

0032-3861/$ - see front matter © 2006 Elsevier Ltd. All rights reserved.
doi:10.1016/j.polymer.2006.04.036

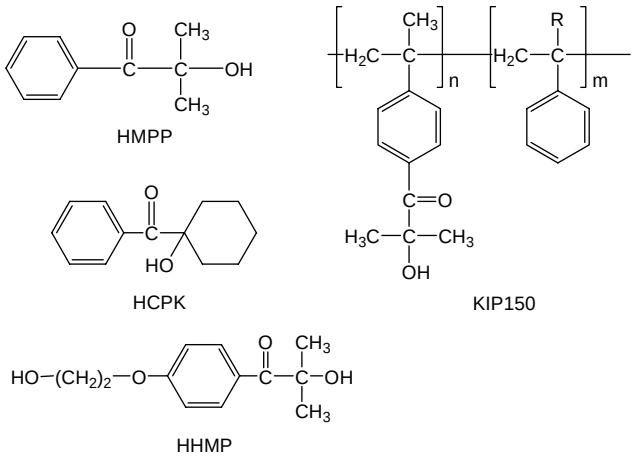

Scheme 1. The structure of some commercial α-hydroxyalkylphenone photoinitiators.

synthesized, which was expected to improve the migration problem while keep relatively high activity in photoinitiation.

2. Experimental

2.1. Materials and methods

Diphenyl ether was recrystallized before used. Anhydrous aluminum chloride, α-chloroisobutyryl chloride and tetra-*n*-butylammonium hydrogen sulfate (TBAHS) were used without further treatment. All of them were from Aldrich. Solvents utilized were dried and redistilled before used. Trimethylolpropane triacrylate (TMPTA) and 2-hydroxyethyl methyacrylate (HEMA) used here was of industrial grade. Photoinitiators HCPK and HMPP were obtained from Runtec Chemical Co. Ltd (Jiangsu, China).

2.2. Synthesis and characterization

The synthesis was conducted following the synthetic route shown in Scheme 2, and detailed characterization had been made for intermediates and the target product.

2.2.1. Acylation of diphenyl ether by Friedel–Crafts reaction

Sixty eight grams (0.4 mol) of diphenyl ether, 113 g (0.85 mol) of aluminium chloride and 300 mL of cyclohexane were mixed together. Eighty nine grams (0.84 mol) of α-chloroisobutyryl chloride was then added dropwise under vigorous stirring. The reaction mixture was stirred at 40–50 °C for further 4 h. The mixture was treated with dilute sodium hydroxide solution, extracted with CH_2Cl_2, dried over anhydrous sodium sulfate, concentrated, and crystallized in hexane. Bis[4-(2-methyl-isopropionyl)-phenyl]ether (I): FT-IR (KBr pellet, cm^{-1}): 3071 (ν aromatic C–H), 2933, 2878 (ν CH_2, CH_3), 1680 (ν C=O), 1588, 1499 (ν aromatic), 1382 (δ, CH_3), 1157 (ν C–O–C); ^{1}H NMR (300 MHz, $CDCl_3$, δ ppm): 1.24 (d, 12H, J= 6.9 Hz, CH_3), 3.52 (m, 2H, J=6.9 Hz, CH adjacent to carbonyl group), 7.06 (d, 4H, J=8.7 Hz, aromatic CH close to ether oxygen atom), 7.97 (d, 4H, J=8.7 Hz, aromatic CH close to carbonyl group); ^{13}C NMR (300 MHz, $CDCl_3$, δ ppm): 19.6 (CH_3), 35.5 (CH), 119.0 (aromatic CH near C–O–C group), 130.8 (aromatic CH near C=O group), 132.1 (aromatic carbon adjacent to carbonyl group), 160.1 (aromatic carbon adjacent to ether oxygen atom), 203.0 (C=O), white crystals, mp 40–41 °C.

2.2.2. Bromination of compound (I)

Calculated amount of liquid bromine was added dropwise to a cyclohexane solution of compound I with stirring at 25 °C, and the reaction was continued for 2 h after bromine was whole added. The treatment process of the product was the same as above. Bis[4-(2-bromo-2-methyl-isopropionyl)-phenyl] ether (II): FT-IR (KBr pellet, cm^{-1}): 3071 (ν aromatic C–H), 2976, 2932 (ν CH_2, CH_3), 1674 (ν C=O), 1584, 1499, (ν aromatic C=C), 1387 (δ CH_3), 1160 (ν C–O–C); ^{1}H NMR (300 MHz, $CDCl_3$, δ ppm): 2.04 (s, 12H, CH_3), 7.08 (d, 4H, J=9.0 Hz, aromatic CH close to ether oxygen atom), 8.23 (d, 4H, J= 8.7 Hz, aromatic CH close to carbonyl group); ^{13}C NMR (300 MHz, $CDCl_3$, δ ppm): 32.1 (CH_3), 60.6 (C–Br), 118.6 (aromatic CH near C–O–C group), 130.2 (aromatic C near C=O group), 133.0 (aromatic CH near C=O group) 159.6 (aromatic C near O atom) 195.1 (C=O); Elem. Anal. Calcd for $C_{20}H_{20}Br_2O_3$: C 51.31%, H 4.31%. Found: C 51.37%, H 4.26%, white crystals, mp 85–87 °C.

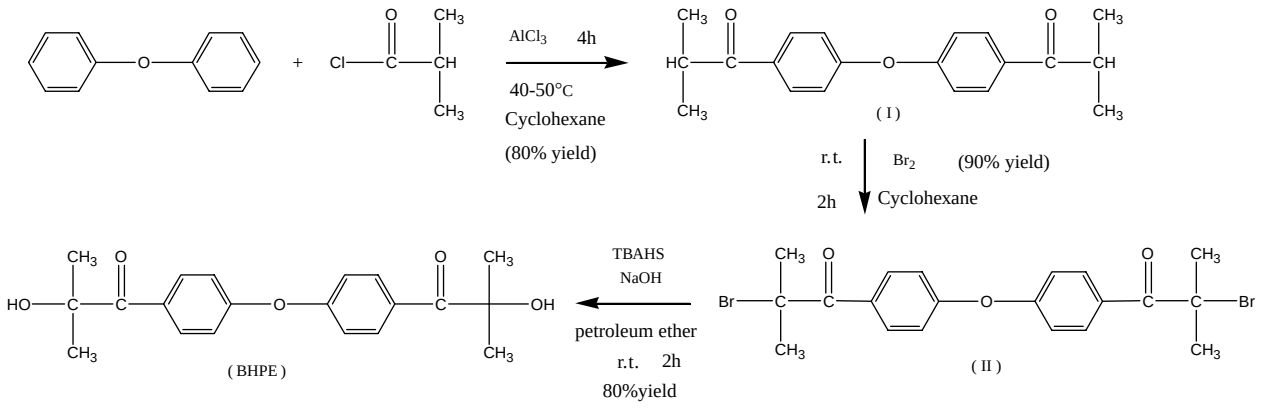

Scheme 2. Synthetic route of BHPE.

2.2.3. Preparation of BHPE from the bromides (II)

The bromide obtained was dissolved in petroleum ether (20 g/L), then mixed with excessive twice folds solution of sodium hydroxide (10 g/L). TBAHS was used as phase transfer catalyst. The mixture was then stirred for further 2–3 h at 25 °C. The deposition was filtrated then recrystallized in hexane. Bis[4-(2-hydroxy-isopropionyl)] ether (BHPE): FT-IR (KBr pellet, cm^{-1}): 3444 (ν OH), 3070 (ν aromatic C–H), 2981, 2931 (ν CH_2, CH_3), 1658 (ν C=O), 1587, 1498, (ν aromatic C=C), 1379 (δ CH_3), 1163 (ν C–O–C); ^{1}H NMR (300 MHz, $CDCl_3$, δ ppm): 1.66 (s, 12H, CH_3), 4.02 (s, 2H, OH), 7.09 (d, 4H, $J=9.0$ Hz, aromatic CH close to ether oxygen atom), 8.12 (d, 4H, $J=8.7$ Hz, aromatic CH close to carbonyl group); ^{13}C NMR (300 MHz, $CDCl_3$, δ ppm): 28.6 (CH_3), 76.8 (quaternary C), 118.8 (aromatic CH near C–O–C group), 129.5 (aromatic C near C=O group), 132.3 (aromatic CH near C=O group), 160.0 (aromatic C near O atom) 202.8 (C=O); Elem. Anal. Calcd for $C_{20}H_{22}O_5$: C 70.16%, H 6.48%. Found: C 69.41%, H 6.37%, white crystals, mp 96–97 °C.

2.3. Physicochemical measurements

FT-IR spectra were carried out on a Thermo Nicolet Nexus™ 670 FT-IR E.S.P. spectrometer (Thermo Electron Co. USA). The samples were prepared either as cast films on KBr discs or as KBr pellets. UV absorption spectra were recorded in CH_2Cl_2 solution on a Varian Cary100 spectrophotometer (Varian Inc., Co. Palo Alto, California, USA). A cell path length of 1.0 cm and concentrations about 10^{-5}–10^{-2} mol L^{-1} were employed. NMR spectra were obtained on a Varian Mercury 300M (Varian Inc., Co. Palo Alto, California, USA) spectrometer. Steady state fluorescence measurements was performed on a FLS920 fluorescence lifetime and steady state spectrometer (Edinburgh Instruments Ltd, Livingston, UK). A xenon lamp (nF900, Edinburgh Analytical Instruments) was used as the excitation source. All emission spectra were recorded using the corrected mode and the fluorescence spectra were recorded with constant slit width. The data of fluorescence lifetime were collected over 200 channels with a time-base of 0.195 ns per channel. Lifetimes were measured by use of a single photon-counting apparatus. The decay data were analyzed using software from FLS 920 based on the biexponential method. The fluorescence quantum yields in nondegassed solutions have been determined using quinine sulfate in 0.05 M sulfuric acid as a reference ($\phi_{fstd}=0.55$).

2.4. Differential photo-calorimetry (DPC)

A modified CDR-1 DSC (Shanghai Balance Instrument Plant, Shanghai, China) equipped with a 125 W middle pressure mercury lamp was employed to measure the exothermal rates of irradiated samples. The light intensity was measured by a UV-radiometer (type UV-A, Photoelectric Instrument Factory, Beijing Normal University, China), which is sensitive in the wavelength range of 320–400 nm. The samples containing 1–5 wt% of the initiator was sonicated for 15 mm to ensure complete dissolving.

2.5. GPC

The molecular weight was investigated by GPC (Breeze GPC, Waters Corp., Milford Massachusetts, USA) with a differential refractive-index detector. THF was used as solvent.

2.6. GC–MS

The photoinitiator was irradiated in CH_2Cl_2 for about 1 h and subjected to GC–MS analysis. The experiment was carried out on a Voyager gas chromatograph (Thermo Finnigan Company, USA). The column was kept at 40 °C for 3 min, then heated to 270 °C at 20 °C/min and maintained 15 min at this temperature. Zone: 3, 200.0 °C, split flow: 20.0, value: 1.00 mL/min.

2.7. TGA

Thermogravimetric analysis (TGA; TG-209C, Netzsch Corp., Selb/Bavaria, Germany) was carried out at a heating rate of 10 °C/min under a nitrogen atmosphere.

3. Results and discussion

3.1. Photophysics properties of BHPE

3.1.1. UV spectra

Fig. 1 shows the absorbance characteristics of different photoinitiators. The absorption maximum of BHPE was at 281 nm, red shifted 37 nm compared to HMPP, dropping into the UVB region. It is suggested that the interaction between the two phenone units via oxygen bridge should cause extension of

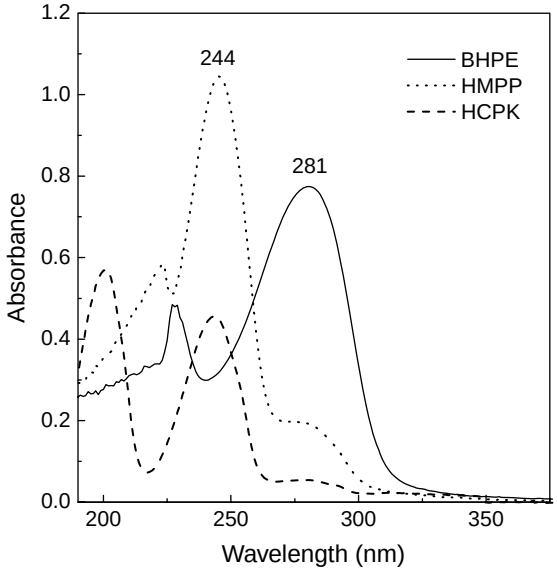

Fig. 1. The UV-vis spectra of photoinitiators in CH_2Cl_2, BHPE (2.3×10^{-5} M), HMPP (8.6×10^{-5} M), HCPK (4.2×10^{-5} M).

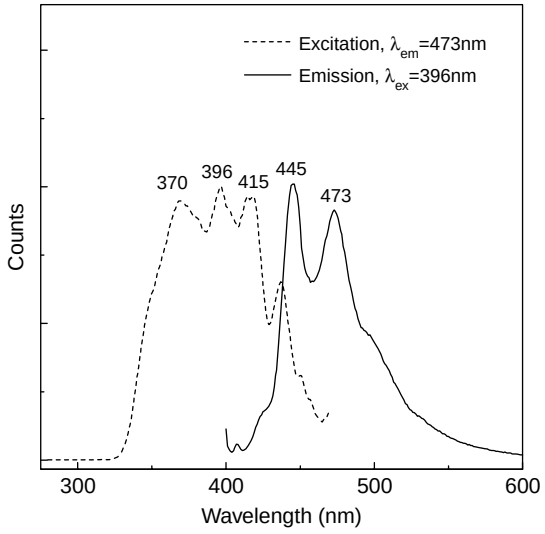

Fig. 2. Fluorescence spectra of BHPE in CH_2Cl_2 (2.3×10^{-5} M0, split = 2 nm.

the conjugation structure, and induce red shift in UV absorption. This absorption character well matches the emission profile of the industrial mercury lamp used in UV coating technology, and thus benefits to improve the photoinitiation efficiency.

3.1.2. Fluorescence

The fluorescence emission spectrum of BHPE in CH_2Cl_2 shows two bands at 445, 473 nm (Fig. 2). The fluorescence lifetime and quantum yield were determined by routine method [14,15]. A multiexponential model was used to improve the fitting of the experimental fluorescence intensity decay data for fluorescence lifetime. The results for BHPE and HMPP are listed in Table 1.

These data show that the singlet lifetimes are very short for the two photoinitiators. The fluorescence quantum yield of BHPE and HMPP were found to be equal to 0.045 and 0.0037 at room temperature, far less than 0.1. The shorter lifetime and lower fluorescence quantum yields of the photoinitiators indicates a rapid depopulation of the singlet excited states by intersystem crossing (ISC). It is consistent with a reduction of the intersystem crossing quantum yield, which reported by Fouassier's group [16]. The triplet states investigation of phenylacetonephenone derivatives by laser spectroscopy found that the intersystem crossing S_1–T_1 was fast since the build up of the triplet state takes place in less than 600 ps. Obviously, for a cleavage type photoinitiator, low fluorescence quantum yield indicates that the photoinitiator is expected to have the advantage of higher cleavage quantum yield, which is directly related to the photoinitiating activity of photoinitiator.

Table 1
Comparison of fluorescence characteristics between HMPP and BHPE

PI	τ_f (ns)	ϕ_f	k_r[a] (s^{-1})	k_{nr}[b] (s^{-1})
BHPE	14.2	0.045	3.2×10^6	6.2×10^7
HMPP	1.9	0.0037	1.9×10^6	5.2×10^8

[a] Radiative deactivation constants, $k_r=\phi_f/\tau_f$ [14].
[b] Non-radiative deactivation constant $k_r=(1-\phi_f)/\tau_f$.

Comparing to HMPP, BHPE has longer singlet lifetime and higher fluorescence quantum yield, implying that the photoinitiating activity of BHPE should be lower than that of HMPP. But, the difference is expected to be limited, for both the singlet lifetime and the fluorescence quantum yield of BHPE are still at very low level.

3.2. Photoinitiating activity

3.2.1. Kinetics studies by DPC

The kinetics of photopolymerization depends on many factors such as choice of photoinitiator, its concentration, the composition of the formulation and functionality of monomers used. It is furthermore affected by various physical factors such as light intensity and wavelength, the thickness of the sample, temperature, etc. For the photopolymerization reaction is exothermic, the polymerization progress can be monitored by means of differential photo-calorimetry (DPC), by which the heat flow (dH/dt) from the sample during irradiation is measured as the function of reaction time (t). The reaction rate is calculated from the reaction enthalpy by the following equation

$$R_p = \frac{d\alpha}{dt} = \frac{d(H/H_\infty)}{dt} = \frac{dH/dt}{i\times H_0} \quad (1)$$

where R_p is the polymerization rate, H_∞, ($=i\times H_0$) the total enthalpy, H_0 the molar enthalpy of C=C bonds in polymerization, and i the mole number of carbon double bond in the system. Conversion curve (α–t) can be obtained by integrating the polymerization rate curve (R_p–t).

The photoinitiating activity of BHPE was tested in comparison with HMPP, as shown in Fig. 3. The sharp rise at the beginning of polymerization indicates the auto-acceleration of the bulk polymerization reaction, which is caused by gel effect. After reaching the maximum polymerization rate, the reaction rate declined as the effect of chain radical embedded. The kinetics can be treated with an auto-catalyzed reaction model phenomenologically, which assumes that at least one of the reaction products is also involved in the propagating reaction. Thus, the reaction rate is expressed by the following equation [17,18]

$$R_p = \frac{d\alpha}{dt} = k\alpha^m(1-\alpha)^n \quad (2)$$

where k is the temperature-dependent kinetic constant defined by Arrhenius theory, m the autocatalytic exponent, n the reaction order, and 1 represents the 100% theoretical conversion. Normally, 100% conversion could hardly be achieved for a photocuring system, in which the polymerization stops ($d\alpha/dt\rightarrow0$) at a limited conversion (α_{max}), because the mobility of the reaction species is seriously restricted by gel effect and the curing reactions become diffusion controlled. So, it is a logical assumption that the 100% theoretical conversion is replaced by practical ultimate

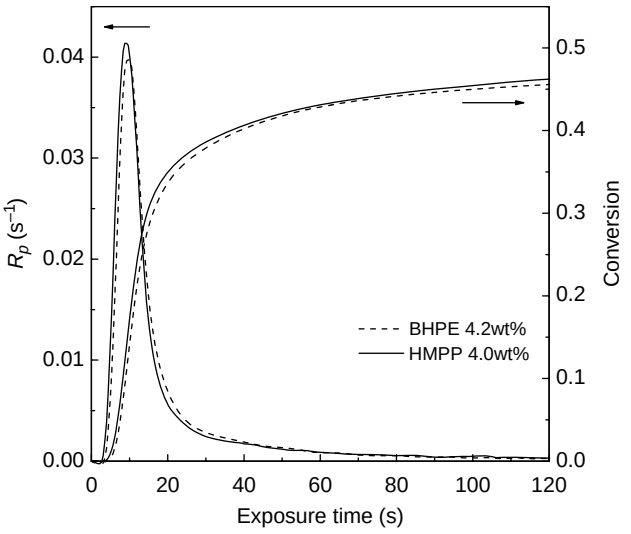

Fig. 3. Conversion vs. exposure time for the photopolymerization of TMPTA initiated by different photoinitiators in N_2, light intensity: 4.0 mM cm^{-2}.

conversion α_{max}, thus Eq. (2) is rewrited as:

$$R_p = \frac{d\alpha}{dt} = k\alpha^m(\alpha_{max} - \alpha)^n \quad (2a)$$

R_p–α curves are obtained from DPC experiments, as shown in Fig. 4. The theoretical curves based on Eq. (2a) are simulated and also shown in the figure. It is found that the simulated curves well match the experimental data. The kinetic analysis results for the photopolymerization are summarized in Table 2. Each of the kinetic parameters is very close for the two photoinitiators.

3.2.2. Bond dissociation enthalpy

To obtain insight into the structural effect on photochemical reactivity of PIs, we have computed the bond dissociation

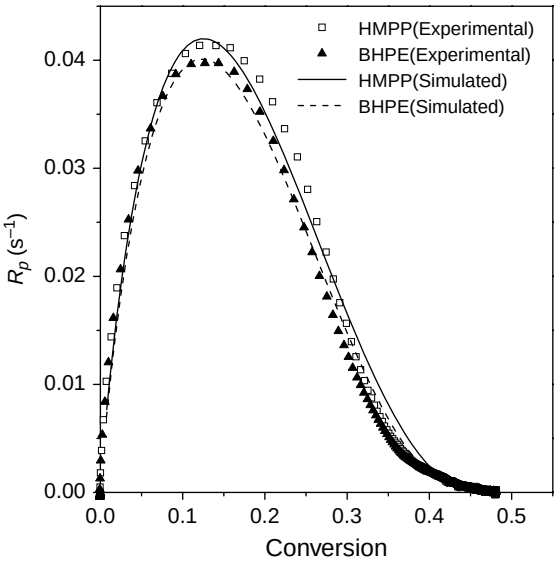

Fig. 4. Plots of the variation of acrylate photopolymerization rate as a function of the conversion at 28 °C.

Table 2
Kinetic analysis results for the photopolymerization

	K	*m*	*n*
HMPP	3.24	0.87	2.33
BHPE	3.10	0.86	2.33

enthalpy in the ground states (S_0) at ab initio level. The result provides quantum chemical information of the PIs that can be compared with the result obtained from experiment. The DFT method and basis set was chose according to Jean–Pierre Fouassier's job [19], because the B3LYP hybrid function leads to the best agreement with the experimental values when associated with an extended basis set such as 6-311++G**

Following these ideas, the bond dissociation energy (DBE) of BHPE was calculated and the results with relative data were summarized in Table 3. Scheme 3 shows the decomposition procedures for the calculation of DBEs. The value (67.84 kcal/mol) was found to be slightly higher than that of HMPP (65.0 kcal/mol) and HCPK (63.5 kcal/mol) [19]. The higher DBE of BHPE is counterbalanced by a red shift in UV absorption character (Fig. 1). The results imply that these photoinitiators have the similar ability on photolysis, resulting in the similar activity in initiating photopolymerization, as shown in Fig. 3.

3.2.3. Quantum yields of initiation and polymerization

The quantum yield of initiation, ϕ_i, is defined as the number of starting chains per photon absorbed and expressed by the following equation [20]

$$R_i = \phi_i I_{abs} \quad (3)$$

where R_i is the rate of initiation, I_{abs} the light intensity absorbed. A simple approach for testing ϕ_i was proposed by Fouassier and co-workers [16], in which ϕ_i of HMPP is used as reference and defined as 100. Thus, the quantum yield of initiation can be obtained from the following equation [16]

$$\phi_i = 100(R_p/R_p^{HMPP})^2 \quad (4)$$

where R_p and R_p^{HMPP} are the polymerization rates for the concerned initiator and HMPP, respectively. To avoid the effect of auto-acceleration, the mono-functional monomer, 2-hydroxyethyl methyacrylate (HEMA), was used. The

Table 3
Calculated DBEs (kcal/mol) of BHPE by B3LYP method and different basis sets

	6-31G*	6-31+G*[a]	6-311++G**[a]	6-311++G**[a,b]
BDE_1	72.60	69.01	67.83	63.31
BDE_2	72.62	69.04	67.83	63.24
BDE	72.61	69.03	67.84	63.28

[a] From computed single point energies using the structures optimized with the 6-31g* basis sets.

[b] Corrected by zero point energies. $BDE_1 = E_{BHPE-1} + E_{Acetone} - E_{BHPE}$, $BDE_2 = E_{Acetone} + E_{BHPE-2} - E_{HMAPO-1}$, $BDE = (2E_{Acetone} + E_{BHPE-2} - E_{BHPE})/2$.

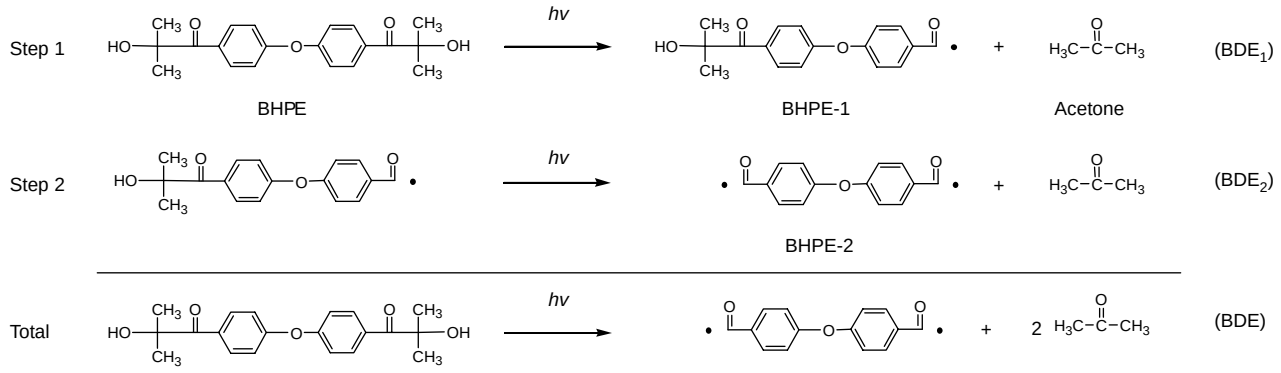

Scheme 3. Decomposition procedures for the calculation of DBEs.

mixture of monomer and initiator was exposed to UV source (315 nm, 1.24 mW s^{-2}) for 30 s, and the reaction heat flow was recorded by DPC. The average reaction rate (R_p) was calculated from the DPC data. By using this method, ϕ_i of BHPE in initiating the polymerization of TMPTA is tested to be 58.

The quantum yield of polymerization, ϕ_m, is defined as the number of monomer units polymerized per photon absorbed and expressed by the following equation [20]

$$\phi_m = \frac{R_p}{I_{abs}} = \frac{R_p}{I_0(1-e^{-2.3\varepsilon[I]l})} \quad (5)$$

where R_p is the polymerization rate in mol L^{-1} s^{-1}, l the layer thickness ($\sim 4\times10^{-2}$ cm), ε the extinction coefficient, [I] the concentration of photoinitiator, I_0/I_{abs} the incident/absorbed light intensity in Einstein L^{-1} s^{-1}. R_p was tested as an average in 30 s exposure by the same way as that for ϕ_i-test. Thus, the quantum yields of polymerization for HMPP and BHPE are tested to be 389 and 296, respectively.

The lower quantum yield of initiation and polymerization for BHPE may be attributed to the coupling of the two free radicals generated by photolysis. The photolysis fragments of BHPE are of less mobility than those of HMPP, thus the free radicals are easier to contact with each other. In the case of photopolymerization of multifunctional monomers such as TMPTA, gelation and auto-acceleration occur at very beginning, so the difference in mobility may be subordinate. Thus, as we have found from Fig. 3 and Table 2, the two photoinitiators have similar kinetic parameters in initiating the polymerization of TMPTA.

3.3. Photolysis mechanism

Though for technical application the improvement of activity is of importance regardless of the mechanism, the understanding of the photolysis mechanism is crucial in view of the continuing effort to improve the efficiency of photoinitiators in order to meet the requirements of new technologies.

Irradiation of BHPE in CH_2Cl_2 induced a continuous shift of the absorption band from 283 to 260 nm in the UV spectra (Fig. 5). One reasonable interpretation for the absorption shift is that the photolysis of BHPE results in the change of the conjugation structure in the molecules. Isoabsorptive point at 270 nm was observed in the UV–vis spectra of BHPE, indicating that photoinitiator photodegradations proceeded selectively without any side reaction [21].

^{1}H NMR spectra of BHPE as a function of the steady-state UV exposure time had been measured for obtaining more information on the photolysis process, as shown in Fig. 6. At the beginning of irradiation, both the ^{1}H NMR spectra showed the decay of original signals (e.g. 1.65 ppm) and the generation of some signals (e.g. 2.05 ppm). After longer irradiation, a new signal at 9.80 ppm was observed.

The signal at 2.05 ppm is assigned to the proton of acetone. It was also confirmed by GC/MS, as shown at Fig. 7 (MS not shown here). The signal at 9.80 ppm is assigned to the proton of CHO, and the possible compound is 4,4′-oxydibenzaldehyde (Scheme 4) [δ = 9.80 ppm (s, 2H, CHO), 7.83 ppm (d, 4H, J =

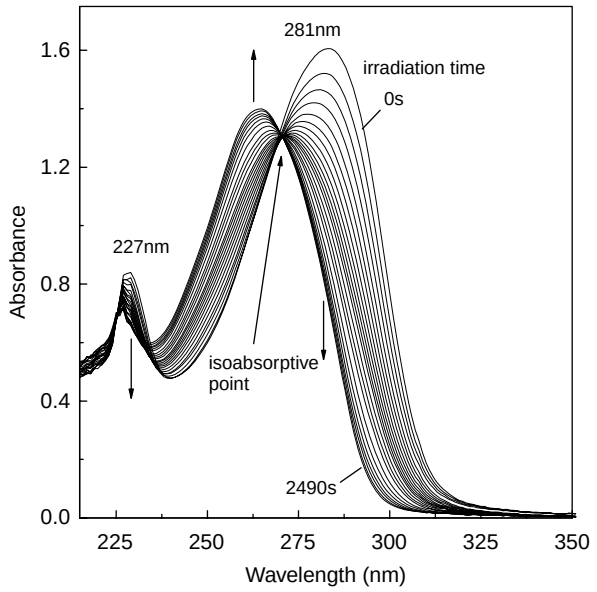

Fig. 5. The UV–vis spectra of BHPE in CH_2Cl_2 (6.0×10^{-5} M) as a function of the steady-state exposure time (from 0 to 600 s with interval of 50 s, then from 690 to 2490 s with interval of 100 s).

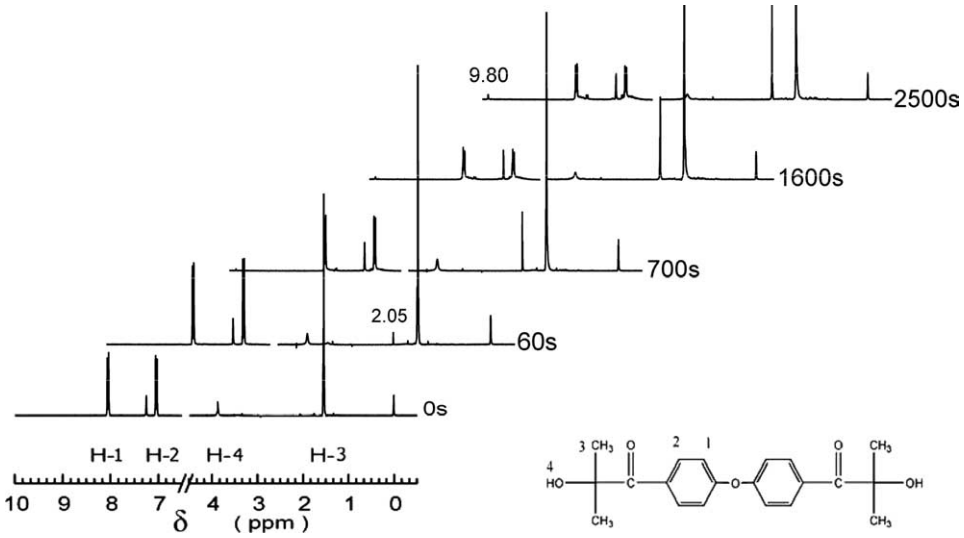

Fig. 6. The ^{1}H NMR signals of BHPE (1 mol/L) in CH_2Cl_2 as a function of the steady-state UV exposure time. CH_2Cl_2 $\delta = 5.30$ ppm, $CDCl_3$ $\delta = 7.26$ ppm.

8.7 Hz, aromatic CH adjacent to CHO group) and 7.10 ppm (d, 4H, $J = 8.7$ Hz, aromatic CH close to ether O atom)]. Fig. 8 shows that, with the increase in irradiation time, the intensities of ^{1}H NMR signal from acetone and –CHO increased, while those from original structure (H-2 and H-3 as marked in Fig. 6) decreased correspondently.

BHPE has similar structure to HMPP. It is well known that α-cleavage (Norrish I) occurs for the photoinitiator of α-hydroxy alkylphenones under UV irradiation [22]. Based on the results obtained in the ^{1}H NMR investigations, it can be concluded that BHPE follows the same photolytic mechanism. The cleavage takes place at the α C–C position of BHPE. Evidence supporting this expectation is based on the result that the acetone and 4,4′-oxydibenzaldehyde were found in the photolytic product. The appearance of acetone is due to the reduction of 2-hydroxy-isopropyl radical. This has been evoked in the article for many acetophone derivatives, and often attributed to the cleavage mechanism (Scheme 3) [23]. Sometimes the effect of oxygen cannot be ignored, a peroxidation mechanism will be observed in the photolysis that consumes the 2-hydroxy-isopropyl radical produced by cleavage. Another evidence is that a remarkable amount of 4,4′-oxydibenzaldehyde was found in the ^{1}H NMR spectra, which is also the α-cleavage product. Because there are two weak bonds in a BHPE molecule, the photolysis will yield

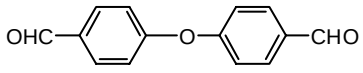

Scheme 4. Structure of 4,4′-oxydibenzaldehyde.

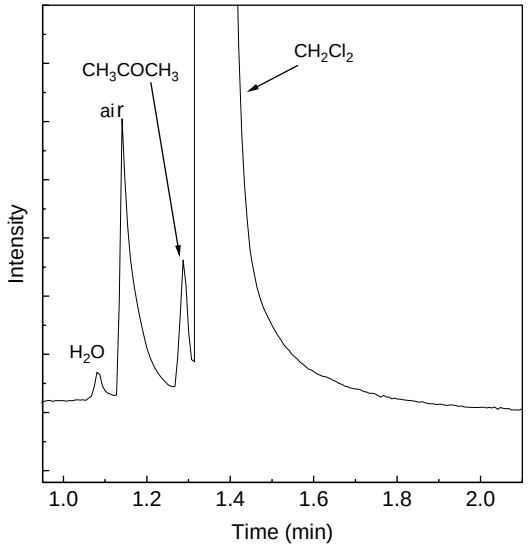

Fig. 7. Photoproducts observed in the GC–MS after photolysis with UV light irradiation for 40 min: GC of photoproduct of BHPE in CH_2Cl_2 (0.01 M).

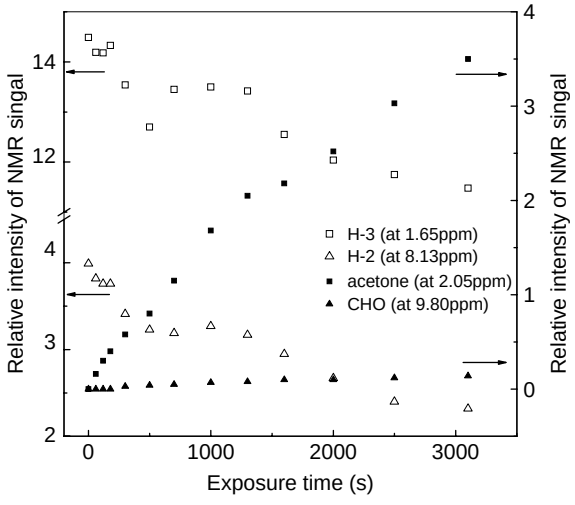

Fig. 8. Relative intensity of the NMR signals as a function of the steady-state UV exposure time for BHPE (1 mol/L) in CH_2Cl_2. TMS was used as internal reference.

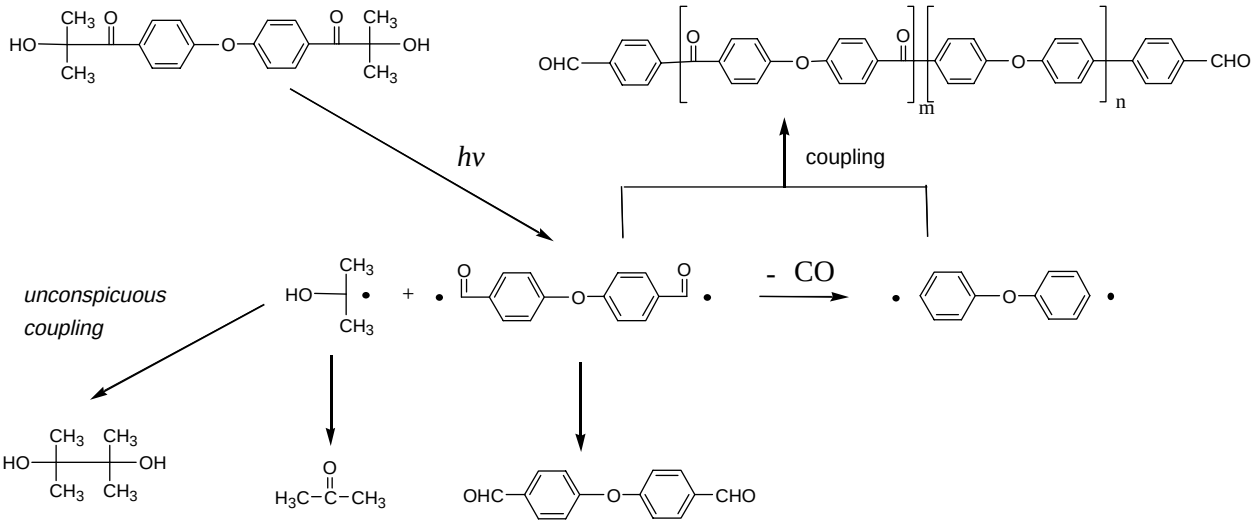

Scheme 5. Proposed mechanism for the photolysis of BHPE.

bis-4, 4′-benzoyl ether radicals (Scheme 5). This radical, which is the precursor of 4,4′-oxydibenzaldehyde, may form directly by single or several steps, but it is more reasonable to believe that it should not be found normally by non-transient method because of its very high activity, or in another word, very short life time. Both of two radicals, bis-4,4′-benzoyl ether and 2-hydroxy-isopropyl radicals, can participate in the initiation process, for example, the bimolecular rate constant k for the reaction of 2-hydroxy-isopropyl radical with MMA was found to be 5.4×10^5 L mol^{-1} s^{-1} [24]. It should be noted that, the volatility is particularly low for 4,4′-oxydibenzaldehyde compared to benzaldehyde, which is the cleavage product of HMPP. So the advantage of low VOCs is expected. Another interesting point is that no other photolysis products could be detected under our experimental conditions. For example, pinacol, which is expected to be the product of coupling between two 2-hydroxy-isopropyl radicals, could not be found by ^{1}H NMR and GC–MS. The phenomenon observed could be associated with the oxygen inhibition to the coupling of the free radicals. Cage effect should also be taken account of, for most of 2-hydroxy-isopropyl radicals are consumed to form acetone in the cage. If there is actually nothing more than 4,4′-oxydibenzaldehyde and acetone in the photoproduct of BHPE, that will be a satisfactory result, for we do not need to worry about the release of other photodecomposition products from the cured matrix, as the acetone is less toxic.

Further investigation to the photolysis mechanism could be attained by directly comparing the molecular weights of BHPE before and after irradiation by GPC, as shown in Fig. 9. Substances with shorter elution time (higher molecular weight) than that of non-irradiation BHPE were found at the front of elution curve, suggesting that coupling between free radicals occurred. Because, there are two free radicals in a photolysis fragment, the coupling reaction may lead to the formation of polymer or oligomer of the fragments. The coupling reaction was reasonable in this case, in which the measurement was carried out in the absence of monomer. Under the practical conditions in which the photoinitiators are surrounded by large amount of monomer or oligomer, the free radicals have great chance to react with carbon double bonds, and the coupling reaction should be ignored.

Based on the above results, the proposed photolysis process for BHPE may be summarized in Scheme 5.

3.4. Volatility

Photoinitiators, which are not totally consumed during the curing process, especially in the deep layer of coating, may volatilize to the atmosphere. With the aim of evaluating the behavior of the photoinitiator under tropical outdoor conditions and to quantitate its volatile degree, a

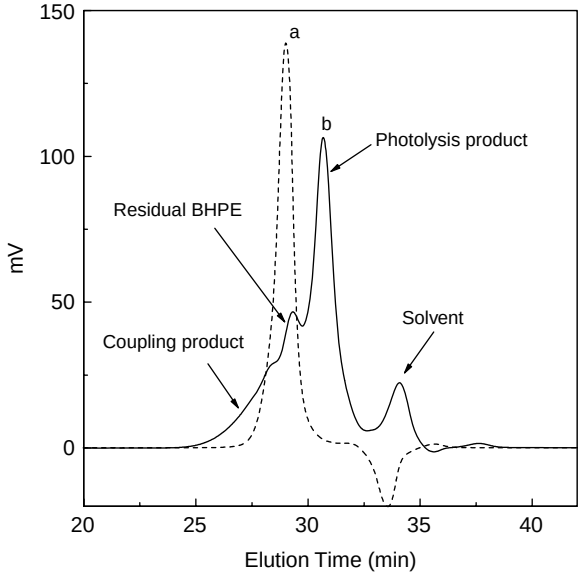

Fig. 9. The GPC traces of photolysis product (BHPE) in THF. (a) Nonirradiation; (b) irradiation for 40 min.

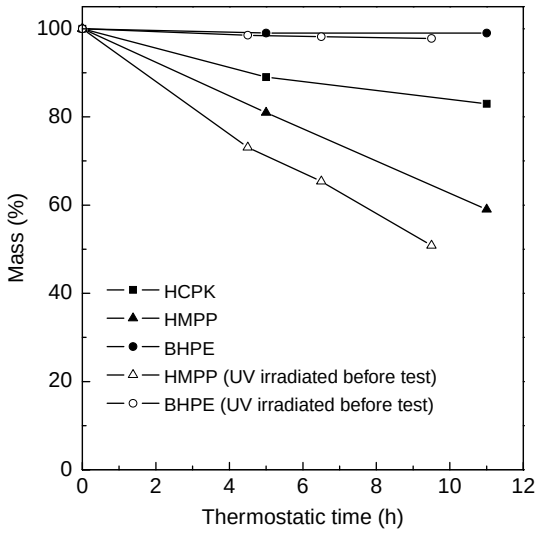

Fig. 10. Plot of residual mass of PIs vs. time at constant temperature (60 °C in air atmosphere).

simple method was adopted. We simulated the situation in which the used materials were exposed to sunlight in summer. The results are shown in Fig. 10. It was found that after storage for 10 h at 60 °C, BHPE and its irradiated samples, which were obtained by exposed to UV light for about one minute before test was practically not released, while weight loses about 40 and 15% were found for HMPP and HCPK, respectively. The photolysis products of HMPP also showed high weight loss in the test. Thus, very low volatility can be expected for BHPE when applied to UV-curing formulation.

Similar results were also found from thermogravimetric analysis (Fig. 11). At temperature lower than 180 °C, no obvious weight loss occurred for BHPE and its irradiated sample, while over 98% of weight loss was found for HMPP and its irradiated sample. The excellent thermal stability of BHPE means less volatility, which is beneficial to the environmental protection and olfaction aesthetic effect while used as photoinitiator in UV-curable coatings for the decoration of goods package.

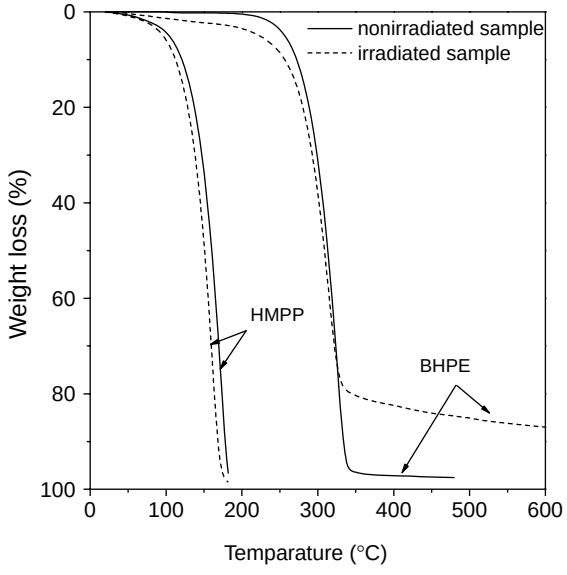

Fig. 11. TG curves for HMPP and BHPE in N_2 at heating rate of 10 °C/min.

In additional investigation it has been found that the solid BHPE was readily soluble in various acrylate monomers, such as triethylene glycol diacrylate (TEGDA) and propylene glycol diacrylate (DPGDA). Besides, the yellowing properties of the two photoinitiators (BHPE and HMPP) are very similar.

4. Conclusion

The synthesized bifunctional photoinitiator (PI), bis[4-(2-hydroxy-isopropionyl)] ether (BHPE) showed photoinitiating activity comparable to the corresponding commercial photoinitiator. The most important aspect is the very low volatility of this photoinitiator as well as its photolytic products. Results showed that BHPE is a promising candidate as a photoinitiator with reduced VOC emission. Work directed to the evaluation of the potential application of this photoinitiator system in related areas is in progress.

Acknowledgements

This work was supported by the National Natural Science Foundation of China (Grant No. 60378029), which is gratefully acknowledged.

References

[1] Decker C. Polym Int 1998;45(2):133–41.
[2] Carlini C, Angiolini L. Adv Polym Sci 1995;123:127–214.
[3] Angiolini L, Caretti D, Carlini C, Corelli E, Salatelli E. Polymer 1999;40:7197–207.
[4] Xuesong J, Hongjie X, Jie Y. Polymer 2004;45(1):133–40.
[5] Decker C, Keller L, Zahouily K, Benfarhi S. Polymer 2005;46(17):6640–8.
[6] Grotzinger C, Burget D, Jacques P, Fouassier JP. Polymer 2003;44(13):3671–7.
[7] Segurola J, Allen N, Edge M, Roberts I. Polym Degrad Stab 1999;65:153–60.
[8] Schafer KJ, Hales JM, Balu M, Belfield KD, Van Stryland EW, Hagan DJ. J Photochem Photobio A: Chem 2004;162:497–502.
[9] Jockusch S, Landis MS, Freiermuth B, Turro NJ. Macromolecules 2001;34:1619–26.
[10] Jockusch S, Turro NJ. J Am Chem Soc 1999;121:3921–5.
[11] Eichler J, Herz CP, Naito I, Schnabel W. J Photochem 1980;12:225–34.
[12] Fouassier JP. Prog Org Coat 1990;18(3):229–52.
[13] Hu S, Popielarz R, Neckers DC. Macromolecules 1998;31(13):4107–13.
[14] Ammara H, Fery-Forguesb S. Dyes Pigments 2003;57:259–65.
[15] Crosby GA, Demas JN. J Phys Chem 1971;75(8):991–1024.
[16] Fouassier JP, Ruhlmann D, Graff B, Morlet-Savary F, Wieder F. Prog Org Coat 1995;25:235–71.
[17] Chandra R, Soni K. Prog Polym Sci 1994;19:137–85.
[18] Lecamp L, Youssef B, Bunel C, Lebaudy P. Polymer 1999;40:1403–9.

[19] Allonas X, Lalevée J, fouassier JP. J Photochem Photobio A: Chem 2003; 159:127–33.
[20] Fouassier JP. Photoinitiation, photopolymerization, and photocuring-fundamentals and applications. Cincinnati: Hanser/Gardner Publications Inc.; 1995 pp. 9–14.
[21] Sarker AM, Sawabe K, Neckers DC. Macromolecules 1999;32:5203–9.
[22] Gruber HF. Prog Polym Sci 1992;17:953–1044.
[23] Dietliker K. In: Oldring PKT, editor. Chemistry and technology of UV and EB formulation for coating, inks and paints, vol. 3. London: SITA Technology; 1991. p. 143–69.
[24] Degirmenci M, Hizal G, Yagci Y. Macromolecules 2002;35: 8265–70.